Optik - International Journal for Light and Electron Optics 270 (2022) 170049

Contents lists available at ScienceDirect

Optik

journal homepage: www.elsevier.com/locate/ijleo

Time-to-frequency conversion method for tunable diode laser absorption spectrum

Xiao Lin [a,b], Meirong Dong [a,b,*], Wei Nie [a,b], Gangfu Rao [a,b], Jidong Lu [a,b]

[a] School of electric power, South China University of Technology,Guangzhou, Guangdong 510640, China
[b] Guangdong Province Engineering Research Center of High Efficient and Low Pollution Energy Conversion, Guangzhou, Guangdong 510640, China

ARTICLE INFO

Keywords:
Direct absorption method
Dynamic wavelength tuning characteristics
Time-to-frequency Conversion method

ABSTRACT

The dynamic wavelength tuning characteristics of the laser is one of the most important factors affecting the measurement accuracy of Tunable Diode Laser Absorption Spectroscopy (TDLAS) technology. We propose a time-frequency conversion method to obtain accurate measurement spectrum, which uses experimentally measured direct absorption signal (time domain) of standard methane gases to compare with simulated spectrum (frequency domain) from the HITRAN database. Then, a polynomial model is used to establish the relationship between time domain (sample points) and frequency domain (wavenumber). To verify the feasibility and accuracy of the method, the methane absorption signals of three standard concentrations (5%, 10% and 15%) were time-to-frequency converted by our method and etalon, and the methane concentrations were calculated and compared. Comparing methane concentration results, the maximum relative error between our method and etalon is less than 0.5%. The results showed that it is viable to use this method to achieve dynamic wavelength measurement in fast scanning of distributed feedback lasers (DFB), and the restricted polynomial model can properly describe the dynamic wavelength tuning characteristics of lasers. Furthermore, the method has the advantages of high accuracy and low cost, which is important for improving the accuracy of TDLAS technology applications.

1. Introduction

Tunable laser absorption spectroscopy (TDLAS) is an optical method for the rapid detection of gases by detecting the isolated absorption line of the molecule, with the narrow line width and fast tuning characteristic of a semiconductor laser. This optical method is characterized by fast measurement speed, high sensitivity, and selective measurement [1], which is often used for accurate measurement in fields such as combustion diagnostics [2,3], environmental monitoring[4,5], and greenhouse gas sensing [6,7]. Laser absorption spectroscopy has great potential for achieving multi-parameter measurements (including temperature, pressure, velocity, component concentration and etc.) [8]. Researchers have developed TDLAS to be a popular analysis method for highly sensitive detection of trace gases through signal-to-noise ratio enhancement techniques (both signal enhancement techniques and noise reduction techniques) [9]. In the detection of complex flow environments, fast frequency scanning is more suitable to reflect real parameter changes. The scanning frequency affects the range of current tuning, which in turn affects the range of wavelength tuning. In the practical application, the detection signal is a time-amplitude signal obtained from the TDLAS system, where the horizontal coordinate of the absorbed signal is the number of sample points, corresponding to the time series. The normalization of the line area is

* Corresponding author at: School of electric power, South China University of Technology,Guangzhou, Guangdong 510640, China.
E-mail address: epdongmr@scut.edu.cn (M. Dong).

https://doi.org/10.1016/j.ijleo.2022.170049
Received 24 June 2022; Received in revised form 27 September 2022; Accepted 27 September 2022
Available online 28 September 2022

only valid in the wavelength domain [10]. A time-to-frequency conversion is therefore required for the fast-tuned TDLAS measurement spectrum.

The tuning characteristic of a diode lasers refers to the regularity of the spectral characteristics of the laser that changes with the tuning circuit and the operating temperature [11], and the wavelength characteristic is one of the tuning characteristics [12]. Researchers have found a nonlinear relationship between optical frequency and tuning signal for most tuned lasers [13], so it is necessary to understand the wavelength tuning characteristics of the laser before calculating the integrated absorbance of the absorption peak. Furthermore, some researchers have worked on the linearization of wavelength scans to improve the resolution and signal-to-noise ratio of the spectra in order to facilitate parameter calculations [14].

Actually, there are various methods for measuring laser frequency and wavelength, including laser frequency measurement methods based on harmonic optical frequency chains[15,16], optical frequency interval dichroism [17], optical frequency combs [18–20], etc. Moreover, laser wavelength measurement method based on the interference principle is also an important wavelength calibration method, and the current instruments with high accuracy developed based on the interference principle can be mainly divided into three kinds: Fizeau etalon [21,22], Michelson interferometer [23], and Fabry-P é rot etalon[24]. What's more, the commercial wavelength meter is also an instrument for high-precision measurement of laser wavelength based on interferometer elements, which can accurately obtain the specific wavelength of the laser being measured and has been proven to be used for optical measurements in different wavelength bands[25,26]. Li et al. [27] achieved wavelength calibration of a DFB laser with a central wavelength near 1573 nm using a wavelength meter(Burleigh, WA-1500-NIR). Wakim et al. [28] established an accurate wavelength meter based on Michelson interferometer, where the unknown wavelength can be determined by the Doppler frequency shift of the output beam of the Michelson interferometer with an accuracy of 6.4×10^{-8}. Owing to the relative complexity and high development cost of the above wavelength measurement methods, the Fabry-P é rot etalon is commonly used for wavelength calibration, which is relatively inexpensive and simple to use. Lu et al. [29] combined an F-P interferometer with a CCD image receiver and combined multiple F-P etalons into a standard set to achieve wavelength measurements in the 38 nm wavelength range.

It is worth noting that the etalon would be affected by environmental disturbances and system noise during the measurement process, while the accuracy of the peak detection algorithm is one of the reasons affecting the accuracy of the time-to-frequency conversion [30]. On the other hand, the refractive index of the etalon is different for different wavelengths of laser, so the refractive index needs to be recalculated for each change of calibration wavelength, while different wavelengths require etalons of different materials. Furthermore, it is important that both the etalon and wavelength meter have a limited wavelength measurement range, and if you want to obtain wavelength information of different wavelength bands, instruments corresponding to the wavelength bands are required. In spite of the fact that the etalons are relatively inexpensive compared to the previous wavelength calibrators, it is not easy for a laboratory to prepare multiple etalons for different wavelength bands.

It is an economical and effective method to combine experimental measurements with the database to replace the etalon for time-to-frequency conversion. Zhu et al. [31] used the HITRAN database to calibrate the spectral frequency domain and selected three characteristic points in the spectrum to obtain the quadratic polynomial curve equation for the time-frequency conversion. Liu et al. [32] proposed a fiber delayed self-heterodyne interferometer (FDSHI) measurement scheme to investigate the dynamic wavelength characteristics of DFB lasers using the quantitative functional relationship between the beat frequency signal and the wavelength tuning amount to calculate the dynamic wavelength value of laser tuning. The work can enable fast measurements of dynamic wavelength characteristics under current tuning of DFB lasers. All the above time-to-frequency conversion methods for wavelength measurements frequently require the use of multiple absorption peaks in the scanning range of the laser, which corresponds to the HITRAN database in order to establish a functional relationship. However, due to the limitations of the scanning range of DFB lasers, the situation where only one absorption line exists is often encountered. The method above is not suitable for the case where only one absorption peak can be measured in the laser scan range. Therefore, it is important to propose a time-frequency conversion method that is applicable to the existence of only a single absorption peak in the scanning range of the laser.

It is crucial to select the suitable model to describe the dynamic wavelength tuning characteristic of tunable diode lasers by the time-to-frequency conversion method. Li et al. [33] established a linear function between the sample points where the two absorption peaks in the direct absorption signal are located and the wavenumber of the corresponding absorption peaks in the HITRAN database. Some another researchers believe that the sample point is non-linearly related to the wavelength correspondence [34–36]. Schlosser et al. [37] obtained the dynamic tuning curves of the laser by etalon measurements and presented a quadratic polynomial relationship between the dynamic tuning wavenumber and the scan time. They also utilized etalons with different lengths of air spacing for determining the dynamic wavelength tuning characteristics and their deviations from linearity, and performed primary and quadratic polynomial fits to the tuning curves, respectively. By comparing the residuals, it was found that the quadratic polynomial fit was more suitable for describing the dynamic wavelength tuning characteristics [38].

To study the dynamic wavelength characteristics of the tunable diode laser, we proposed a time-to-frequency conversion method to measure the absorption spectral of methane standard gas by direct absorption without the use of etalons. By comparing the measured absorption spectrum and the simulated spectrum of methane, a time-frequency conversion model between the sample points and wavenumber is developed. The model could realize the time-frequency conversion in the presence of only one gas absorption peak in the tuning range of the laser. Finally, the measurements were applied to different methane concentrations (5%, 10% and 15%) to verify the variability between the model and commercial standard instruments.

2. Methods and experimental

2.1. TDLAS measurement principle

Wavelength scanning-direct absorption TDLAS is a measurement technique based on the selective absorption of gas molecules. The scanning wavelength-direct absorption method tunes the wavelength of the DFB laser by controlling the current and temperature. The absorption spectrum is based on the Beer-Lambert law, which relates the incident laser intensity I_0 to the transmitted laser intensity transmitted through a homogeneous gas medium :

$$\left(\frac{I_t}{I_0}\right) = \exp\left(-\alpha_\nu\right) = \exp\left(-PS(T)x_{abs}\phi_\nu L\right) \tag{1}$$

where α_ν is the spectral absorbance at frequency ν, P[atm] is the absorbing species pressure , x_{abs} represents the molar fraction of the species and is a line function, L[cm] is the absorption path length, and $S(T)$[$cm^{-2}atm^{-1}$] is the temperature-dependent line strength of line.

When wavelength scanning-direct absorption spectroscopy is performed, the signal generator produces a sawtooth voltage waveform at a given repetition frequency, so that the laser is continuously scanned around the central frequency to form a laser beam with an emitted light intensity. The laser beam passes through the gas cell to be measured after the collimator, and the absorption signal after passing through the gas cell to be measured is the transmission signal, which is received by the photodetector and sent to the computer via the data acquisition card.

The integrated absorbance A of the gas can be obtained by processing the transmission signal of the absorption spectrum.

$$A = PS(T)x_{abs}L \tag{2}$$

When calculating the concentration of the target component, the molar fraction of the substance x_{abs} on the absorption path can be calculated using the Eq. (3).

$$x_{abs} = A/PS(T)L \tag{3}$$

2.2. Time-to-frequency conversion method

Taking methane gas as an example, there is only one absorption peak near its absorption line located at 6046 cm^{-1}, and it is impossible to establish the time-frequency function according to the central wavelength of different absorption peaks. In order to solve this issue, time-frequency conversion calculation method was proposed based on the restricted polynomial model. Since the wavenumber obtained by the method of wavelength calibration using experiment has the same resolution as the actual measured spectrum, and the response rate is consistent with the laser frequency, the measurement results are closer to the actual wavelength distribution.

The absorption spectrum of methane was obtained by direct absorption measurements, and the horizontal coordinate of the spectrum in the actual measurement process is the sample points x representing time. According to the measurement conditions (temperature, pressure, optical range length, gas type, concentration, etc.) in the actual measurement process, the theoretical absorption spectrum can be obtained based on the HITRAN database. For gaseous molecule absorption, the linear function may be represented by a Lorentz function when only the collision effect dominates, a Gaussian function when the Doppler effect is dominant.

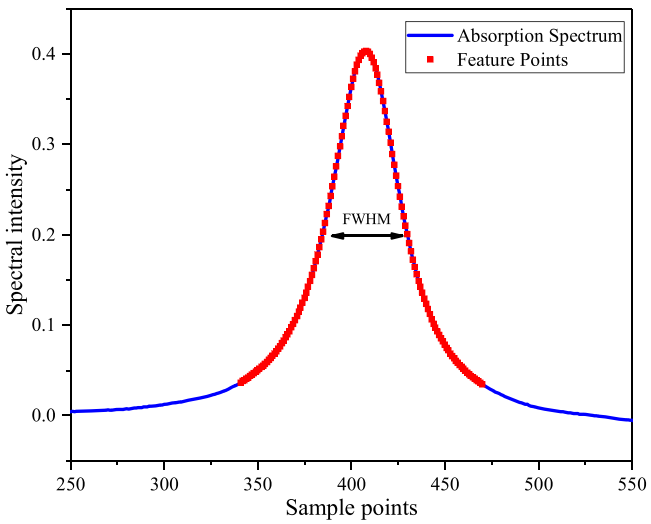

Fig. 1. Methane absorption spectrum and the feature points selected.

When both effects are important, the line shape function can be expressed by the voigt function. Therefore, we used the voigt line function to fit the absorption spectra obtained from the HITRAN in order to get the theoretical spectrum. The horizontal coordinate of the theoretical spectrum is the wavenumber information ν representing frequency. We make a comparison between the measured spectrum and the theoretical spectrum, then set the points with the same spectral intensity as the feature points, so that multiple feature points can be selected in the absorption peak range, as shown in Fig. 1. It's worth noting that, the absorbance intensity at the wings of the experimentally measured methane absorption spectrum is weak, and the absorption spectrum intensity, noise and environmental factors affect the signal-to-noise ratio of the direct absorption spectrum. To avoiding the time-to-frequency conversion model affected by the uncertainty of the wing of absorbance spectrum, the points with spectral intensity less than one-tenth of the peak spectral intensity will be eliminated when selecting the feature points. By corresponding the horizontal coordinates of the same feature point in the actual measured spectrum and the theoretical spectrum, we can plot the sample point-wavenumber correspondence of the measured spectrum, as shown in Fig. 2.

It can be used to establish the function between sample points and wavenumber. To investigate the suitable model for describing the time-frequency conversion relationship, linear model and quadratic polynomial model $\nu = f(x)$ are developed under the conditions of theoretical spectral absorption peak FWHM and integrated absorbance, respectively. Since the full width at maximum (FWHM) and the integrated absorbance of the direct absorption spectrum contain information about the gas type, concentration, ambient temperature, pressure and optical range length of the measurement conditions, it is necessary to consider these restrictions when establishing the sample points-wavenumber function relationship of the feature points. By obtaining the theoretical FWHM of the spectrum as well as the central wavenumber of the theoretical spectrum through the HITRAN database, the following restrictions can be established.

$$\mathrm{FWHM}=\nu_2-\nu_1=f(x_2)-f(x_1) \tag{4}$$

$$\nu_{peak}=f(x_{peak}) \tag{5}$$

where ν_1,ν_2 are the absolute wavenumbers at the ends of the half height of the theoretical spectrum, x_1,x_2 are the sample points at the ends of the half height of the measured spectrum. ν_{peak} and x_{peak} are the central wavenumber of the theoretical spectrum and the central sample points of the measured spectrum, respectively.

Notably, the error of methane gas concentration is about ± 1%. In the case of the 5% standard concentration of methane gas used in the experiment, the actual concentration range is 4.95%− 5.05%. Based on the experimental conditions, methane simulation spectrums were obtained in the HITRAN database, where 5% concentration methane simulation spectrums served as the control group, 4.95% and 5.05% concentration methane simulation spectra served as the experimental group, as shown in Fig. 3.

The feature points are selected separately based on the method proposed in this paper. Fig. 4(1) shows the feature points of the control group and the experimental group respectively; Fig. 4(2) shows the relative error between the feature points of the experimental group and the control group. As shown in Fig. 4, although there is ± 1% error in methane gas concentration, the relative error between the selected feature points of the experimental group and the control group are less than 0.02%. With the restraints of integrated absorbance and FWHM, the errors are not enough to affect the accuracy of the quadratic polynomial model.

2.3. Experimental setup

Fig. 5 shows the layout and schematic diagram of the experimental setup for wavelength scanning-direct absorption spectroscopy. The system used a DFB laser as the laser source, and the DFB laser emits a scanning laser, which had different wavelengths at different

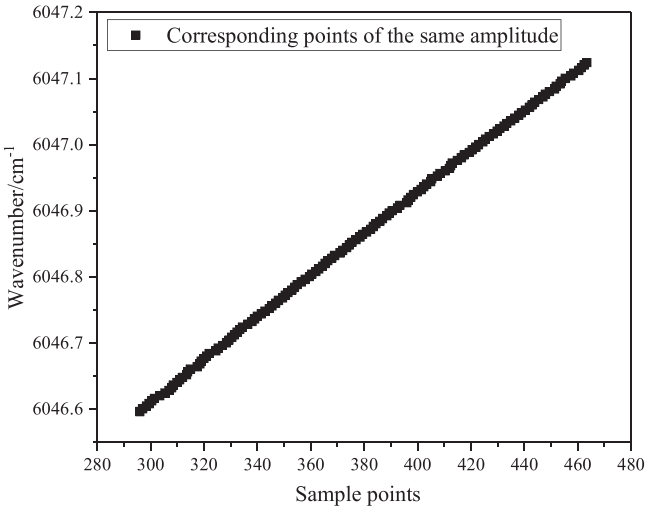

Fig. 2. Sample points-wavenumber correspondence diagram.

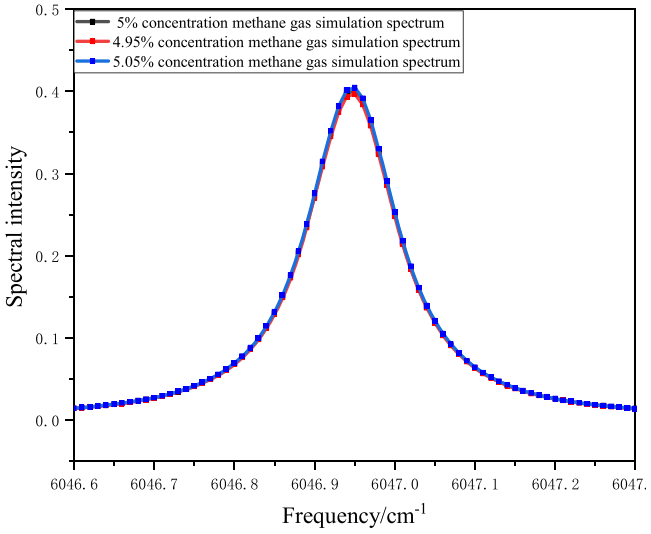

Fig. 3. methane simulation spectrums of 4.95%, 5% and 5.05% concentration.

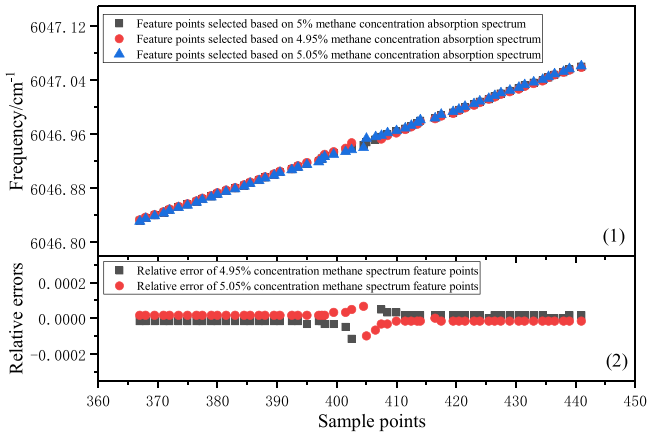

Fig. 4. (1) The feature points of the control group and the experimental group; (2) The relative error between the feature points of the experimental group and the control group.

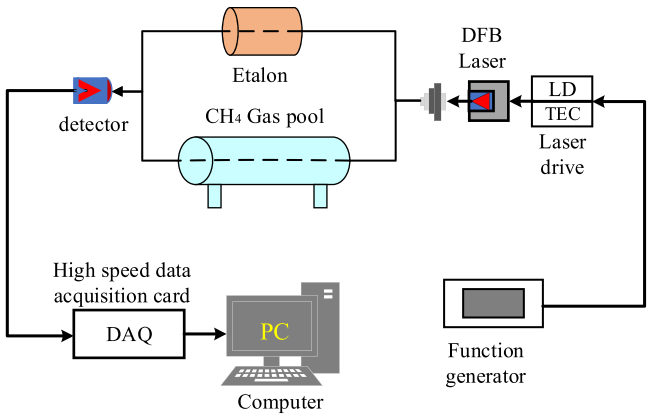

Fig. 5. System diagram of the experimental setup.

moments in the scanning period. The DFB laser selected for this experiment has only a methane gas absorption peak centered at 1653.7 nm (6046.95 cm^{-1}) in the scanning range. DFB laser is wavelength tuning by fixed operating temperature and tuned by adjusting the injection current. In the actual measurement, a function generator was used to generate a saw-tooth wave current to make the laser output a continuous laser with a certain wavelength centered on the laser. The beam was splitted after laser output, one beam was received by the detector after passing through a cell filled with a certain concentration of methane to obtain a laser attenuation signal, and the other beam was passed through the etalon to generate an interference signal for time-to-frequency conversion. The detector signal is collected by the data acquisition module after passing through the transimpedance amplifier circuit.

The experiments were performed at atmospheric pressure and the temperature of 23 °C (296 K), and the methane gas cell was continuously fed with a standard gas of 5% methane concentration and the carrier gas was 95% N_2. The line strength was obtained using the HITRAN database, and the length of the gas cell was 21.5 cm. The absorption line of CH_4 gas at atmospheric temperature and pressure could be collected in real-time by the direct absorption method.

The wavenumber of the 1654 nm DFB laser used in this work was calibrated with an F-P etalon, and the transmission signal of the laser after passing through the etalon is shown in Fig. 4. Since the laser wavelengths emitted by the laser are different at different times, the corresponding transmittance differs when the light of different center wavelengths passes through the F-P etalon, so the transmission signal can be obtained in the form of continuous periodic peaks and valleys after the scanning laser passes through the etalon, Fig. 6(1) shows the transmission signal of the laser passing through the etalon. The distance between adjacent wave peaks is called the free spectral range (FSR)[39,40], with the expression of $FSR = 1/2\ n\Delta L\cos\theta$. The FSR of the etalon used in the experimental system is 0.0693 cm^{-1}. Through the peak detection algorithm to obtain the value of fixed wavelength output time (t_1, t_2, t_3, t_4) in the output spectrum of the etalon, combined with the free spectral range (FSR) of the etalon, we can obtain the correspondence between wavelength and time in Fig. 6(2). The wavelength expressions $\lambda = f(t)$ were subsequently obtained by polynomial fitting.

The wavenumber results from the etalon calibration will be used as a control group for this experiment as a validation. To validate the accuracy of the time-frequency conversion model, we applied this novel method to measurements of different methane concentrations (5%, 10% and 15%) and compared the results with those of commercial etalons.

3. Results and discussion

3.1. Time-to-frequency conversion measurements based on restricted linear model

The restricted linear model was developed according to the sample points-wavenumber correspondence (Fig. 2) under the restrictions of combining the half-height width of the absorption peak of the theoretical spectrum as well as the integrated absorbance condition. The measuring results from the etalon in Section 3.1 were sorted by sample points along the short-wave direction and compared with the developed restricted linear model developed, then the comparison results were plotted in Fig. 7(1), and the absorption spectra were put into the same coordinate system for reference. The wavenumber results measured by the linear model and the etalon are put into the same set of absorption spectra of 5% methane concentration for comparison, as shown in Fig. 7(2).

Although the linear model fits well with the results of the etalon in the region near the absorption peak, as shown in Fig. 7, the model deviates from the results of the etalon in the wavenumber range corresponding to the scanning range of the laser, and the deviation becomes larger and larger as it moves away from the absorption peak. The correlation coefficient (R^2) between the linear model and the etalon results is only 0.8117 and the root mean square error (*RMSE*) is 0.78652. Since it is nonlinear in the dynamic wavelength tuning of the laser, it is not appropriate to describe it using a linear model, so it is need to use a nonlinear model for time-

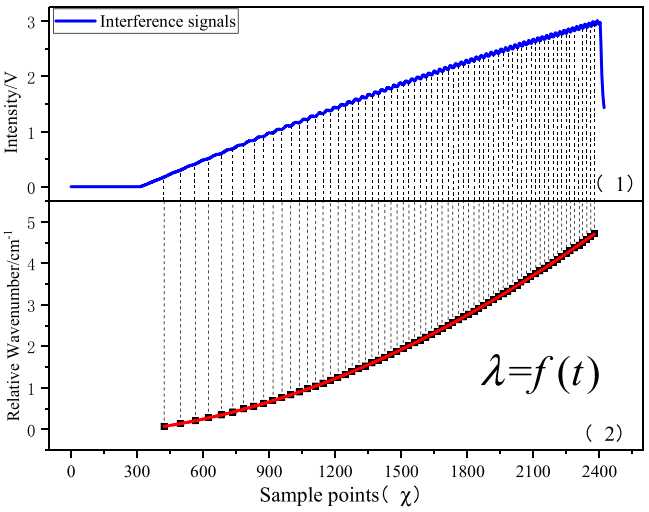

Fig. 6. (1) The interference signal of the laser passing through the etalon; (2) the function relationship of the relative wavenumber and sample points in the scanning range of the DFB laser.

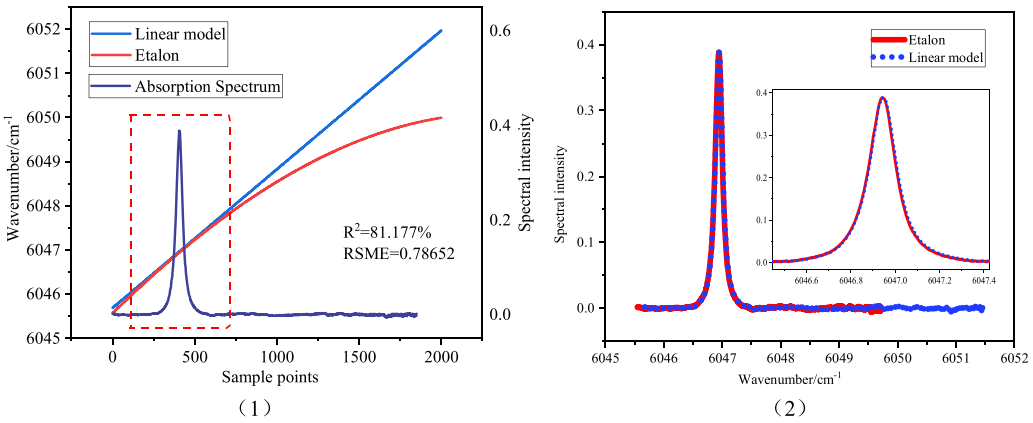

Fig. 7. (1) Time-to-frequency conversion results of linear model (2) Wavenumber-spectrum intensity comparison diagram.

frequency conversion.

3.2. Time-to-frequency conversion measurements based on restricted polynomial model

From the analysis in Section 3.1, it is clear that the linear model is not suitable for describing the time-frequency conversion relationship of the laser, then the restricted quadratic polynomial model is established according to Fig. 2, which can be used to describe the dynamic wavelength tuning characteristics. The results compared with that from the etalon measurement, is shown in Fig. 8.

It can be found that the restricted quadratic polynomial model has good correlation with the etalon results in the region with absorption peaks throughout the laser scanning range, with the correlation coefficient R^2 of 0.9949 and the *RMSE* is only 0.08913, indicating that the model can better describe the wavelength dynamic tuning characteristics of the laser in the scanning range. The lack of computable data in the region outside the methane absorption peak makes it difficult to correct the time-to-frequency conversion relationship in this region, which is the source of the deviation between the calculated frequency results and the etalon measured results in this region. Despite of this, there is also a high correlation between the time-to-frequency conversion model and the results measured by the etalon in the region outside the methane absorption peak. In the DFB laser scanning range of this case, the residuals between the calculated frequency results in the region outside the absorption peak and the frequency results measured by the etalon is less than 0.2.

The restricted model and etalon results were substituted into the absorption spectra of the same set of 5% methane concentration as a comparison, and the wavenumber-spectrum intensity comparisons were obtained in Fig. 9.

The restricted quadratic polynomial model fits well with the spectrum of the etalon in the absorption peak region, and the wavenumber range calculated by the model is close to the results of the etalon. To compare the deviations between the component concentrations calculated by the restricted polynomial models and the etalon result, three sets of standard methane gases with different concentrations were measured with the experimental system, respectively. The methane concentration in the experiment was 5% ± 500 ppm, 10% ± 1000 ppm, and 15% ± 1500 ppm, respectively. The concentration results under each model were calculated according to Eq. (3). The concentration results of the restricted polynomial models and the relative errors were calculated based on the concentrations measured by the etalon as the control group. The relative errors were calculated by the Eq. (6).

$$\delta = |A - A^*|/A \tag{6}$$

where A is the concentration value calculated utilizing the etalon and A^* is the concentration value calculated by the restricted polynomial model. The results and deviations of the concentrations calculated by each measurement method are shown in Table 1.

By comparing the model with the calibration results of the etalon, it was found that the relative error between the restricted quadratic polynomial model and the results of the etalon was less than 0.5% when calculating the gas concentration. The deviation between the model results and the etalon results decreases as the concentration of the measured components increases. The main reason is that as the concentration increases, the signal-to-noise ratio of the absorption spectrum increases, the measurement results become more accurate. It is worth noting that, in Fig. 9 there is some deviation between the time-to-frequency conversion results measured by the restricted polynomial model and the etalon, but the deviation between the two is quite minor when calculating the gas concentrations. That's because the proposed method builds a time-frequency conversion model by comparing the spectral information of the absorption peak regions with the HITRAN database, the frequency information of the regions without absorption peaks can be deduced from the model. What's more, the time-to-frequency conversion model is related to the tuning characteristics of the laser which is not necessarily a quadratic polynomial model. However, at least in this case, the wavelength tuning of the methane laser can be fitted with a quadratic polynomial model. The wavelength tuning characteristics of other lasers may require the use of their corresponding models and further analysis is needed.

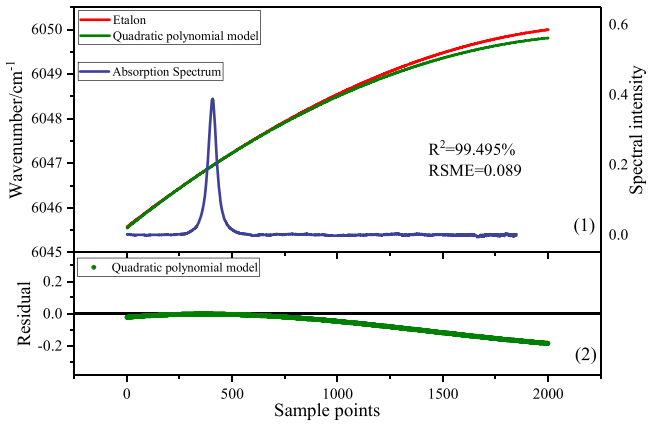

Fig. 8. (1) The restricted quadratic polynomial model (2) The residuals of the quadratic polynomial model.

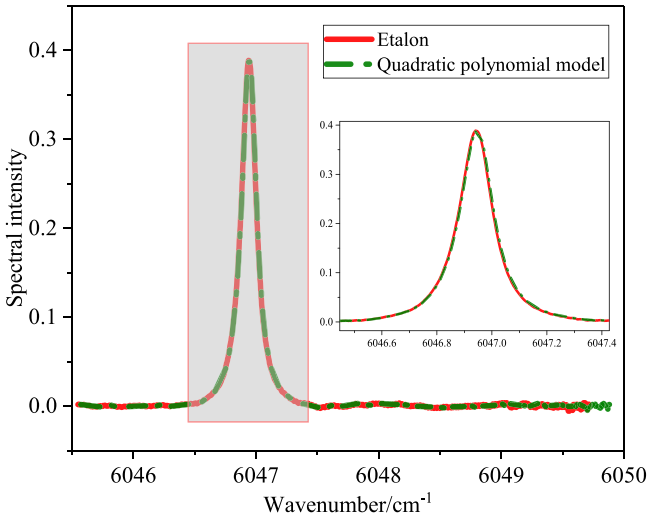

Fig. 9. Comparison of the wavenumber-spectral intensity of the quadratic polynomial model and the etalon.

Table 1
Results and deviations of the measured concentrations of the restricted quadratic polynomial models and the measured concentrations of the etalon.

Experiment serial number	Measurement Method		
	Etalon	Restricted Quadratic polynomial model	
		Results	Relative Error
1	4.92%	4.900%	0.41%
2	9.87%	9.835%	0.35%
3	14.82%	14.77%	0.34%

4. Conclusions

We proposed a method on the accurate time-frequency conversion of the measured spectra of tunable diode lasers. Based on understanding of the dynamic wavelength tuning characteristic of the laser, the time-frequency conversion of TDLAS can be realized by an experimental method. The case where only one absorption peak exists in the scanning range of the laser can be calibrated by this method for wave number calibration. We utilized experimental measurements to obtain the direct absorption spectra of methane standard gases which has only one absorption peak exists in the scanning range of the laser. Comparing the experimentally measured spectra with the theoretical spectra in the HITRAN database, the restricted quadratic polynomial model is established to present the correlation between the time domain sample points and the frequency domain wavenumber. The model can accurately obtain the dynamic wavelength of the DFB laser, where the correlation coefficient is above 0.99, with a relative error of less than 0.5% in the

calculated component concentrations, and the relative error decreases with the increase of the measured component concentration. The developed method has the advantages of high accuracy and simple operation, which is important for gaining insight into the dynamic wavelength tuning characteristic in the scanning range of lasers and improving the detection accuracy of tunable diode lasers, and has great potential for low-cost TDLAS applications.

Funding information

This work was supported by the National Natural Science Foundation of China [No. 51976064]; the Guangdong Basic and Applied Basic Research Foundation [2020A1515010646, 2022A1515010709]; the Fundamental Research Funds for the Central Universities [2022ZFJH004] and the Science and Technology Planning Project of Guangzhou [202102020726].

Declaration of Competing Interest

The authors declare that they have no known competing financial interests or personal relationships that could have appeared to influence the work reported in this paper.

Data Availability

The authors do not have permission to share data.

Acknowledgement

We acknowledge the support from the Guangdong Province Key Laboratory of Efficient and Clean Energy Utilization (2013A061401005).

References

[1] P. Werle, A review of recent advances in semiconductor laser based gas monitors, Spectrochim. Acta Part A: Mol. Biomol. Spectrosc. (1998) 197–236.
[2] L.H. Ma, L.Y. Lau, W. Ren, Non-uniform temperature and species concentration measurements in a laminar flame using multi-band infrared absorption spectroscopy, Appl. Phys. B 123 (2017).
[3] J. Wang, M. Maiorov, D.S. Baer, D.Z. Garbuzov, J.C. Connolly, R.K. Hanson, In situ combustion measurements of CO with diode-laser absorption near 2.3 μm, Appl. Opt. 39 (2000) 5579–5589.
[4] L. Zhang, F. Wang, J. Yan, K. Cen, NO concentration sensing at 1.79μm transition using tunable diode laser absorption spectroscopy, AIP Conf. Proc. 254 (2014) 254–260.
[5] D.T. Cassidy, J. Reid, Atmospheric pressure monitoring of trace gases using tunable diode lasers, Appl. Opt. 21 (1982) 1185–1190.
[6] M. Raza, L. Ma, C. Yao, M. Yang, Z. Wang, Q. Wang, R. Kan, W. Ren, MHz-rate scanned-wavelength direct absorption spectroscopy using a distributed feedback diode laser at 2.3 μm, Opt. Laser Technol. 130 (2020).
[7] V. Nagali, S.I. Chou, D.S. Baer, R.K. Hanson, J. Segall, Tunable diode-laser absorption measurements of methane at elevated temperatures, Appl. Opt. 35 (1996) 4026–4032.
[8] Z. Niu, H. Qi, Z. Zhu, K. Li, Y. Ren, M. He, A novel parametric level set method coupled with Tikhonov regularization for tomographic laser absorption reconstruction, Appl. Therm. Eng. 201 (2022).
[9] J. Li, B. Yu, W. Zhao, W. Chen, A review of signal enhancement and noise reduction techniques for tunable diode laser absorption spectroscopy, Appl. Spectrosc. Rev. 49 (2014) 666–691.
[10] J.F.A. Perlitz, H. Broß, S. Will, Measurement of water mole fraction from acoustically levitated pure water and protein water solution droplets via tunable diode laser absorption spectroscopy (TDLAS) at 1.37 μm, Appl. Sci. 11 (2021).
[11] Z. Du, W. Zhen, Z. Zhang, J. Li, N. Gao, Detection of methyl mercaptan with a 3393-nm distributed feedback interband cascade laser, Appl. Phys. B 122 (2016).
[12] R.J. Lu, D.M. Shen, Q.Q. Du, B.Z. Huang, J.S. Shi, Tuning Characteristics of DFB Diode Laser and its Application to TDLAS Gas Sensor Design, Appl. Mech. Mater. 511–512 (2014) 173–177.
[13] K. Wunderle, S. Wagner, I. Pasti, R. Pieruschka, U. Rascher, U. Schurr, V. Ebert, Distributed feedback diode laser spectrometer at 2.7 microm for sensitive, spatially resolved H2O vapor detection, Appl. Opt. 48 (2009) 172–182.
[14] X. Zhang, J. Pouls, M.C. Wu, Laser frequency sweep linearization by iterative learning pre-distortion for FMCW LiDAR, Opt. Express 27 (2019) 9965–9974.
[15] K.M. Evenson, J.S. Wells, F.R. Petersen, B.L. Danielson, G.W. Day, Accurate frequencies of molecular transitions used in laser stabilization: the 3.39μm transition in CH_4 and the 9.33 and 10.18μm transitions in CO_2, Appl. Phys. Lett. 22 (1973) 192–195.
[16] D.A. Jennings, C.R. Pollock, F.R. Petersen, R.E. Drullinger, K.M. Evenson, J.S. Wells, J.L. Hall, H.P. Layer, Direct frequency measurement of the I_2-stabilized He-Ne 473-THz (633-nm) laser, Opt. Lett. 8 (1983) 136–138.
[17] H.R. Telle, D. Meschede, T.W. Hansch, Realization of a new concept for visible frequency division: phase locking of harmonic and sum frequencies, Opt. Lett. 15 (1990) 532–534.
[18] K. Tong, Z. Du, J. Li, L. Yuan, Optical frequency comb based on a distributed feedback semiconductor laser with direct injection current multi-frequency modulation, Opt. Laser Technol. 137 (2021).
[19] A. Schliesser, N. Picqué, T.W. Hänsch, Mid-infrared frequency combs, Nat. Photonics 6 (2012) 440–449.
[20] T. Udem, J. Reichert, R. Holzwarth, T.W. Hänsch, Accurate measurement of large optical frequency differences with a mode-locked laser, Opt. Lett. 24 (1999) 881–883.
[21] J. Zhang, Y. Zhang, W. Sun, L. Yuan, Multiplexing multimode fiber and Fizeau etalon: a simultaneous measurement scheme of temperature and strain, Meas. Sci. Technol. 20 (2009).
[22] M.B. Morris, T.J. Mcllrath, J.J. Snyder, Fizeau wavemeter for pulsed laser wavelength measurement, Appl. Opt. 23 (1984) 3862–3868.
[23] T.A. Al-Saeed, D.A. Khalil, Characteristics of a refractometer based on Michelson interferometer integrated with a Fabry-Perot interferometer, Optik 242 (2021).
[24] C. Chang, P. Tung, L. Shyu, Y. Wang, E. Manske, Fabry–Perot displacement interferometer for the measuring range up to 100 mm, Measurement 46 (2013) 4094–4099.
[25] H. Deng, J. Sun, B. Yu, J. Li, Near infrared diode laser absorption spectroscopy of acetylene between 6523 and 6587cm−1, J. Mol. Spectrosc. 314 (2015) 1–5.
[26] L. Xu, S. Zhou, N. Liu, M. Zhang, J. Liang, J. Li, Multigas sensing technique based on quartz crystal tuning fork-enhanced laser spectroscopy, Anal. Chem. 92 (2020) 14153–14163.

[27] J.S. Li, K. Liu, W.J. Zhang, W.D. Chen, X.M. Gao, Pressure-induced line broadening for the (30012)←(00001) band of CO_2 measured with tunable diode laser photoacoustic spectroscopy, J. Quant. Spectrosc. Radiat. Transf. 109 (2008) 1575–1585.
[28] M. Wakim, S. Topcu, L. Chassagne, J. Nasser, Y. Alayli, P. Juncar, Highly accurate laser wavelength meter based on Doppler effect, Opt. Commun. 262 (2006) 97–102.
[29] H. Lu, L. Jiang, W. Geng, J. Hong, Study on the real-time measurement of passive incident laser wavelength with F-P interferometers, J. Appl. Opt. 17 (1996) 18–22.
[30] M. Chen, S. Pang, J. Zhou, H. Wu, M. Hirokazu, T. Kiyoshi, High-accuracy spectral interferometer with multi-Fabry–Perot Etalon for thickness measurement of the silicon wafer, Opt. Commun. 501 (2021).
[31] X. Zhu, S. Yao, W. Ren, Z. Lu, Z. Li, TDLAS monitoring of carbon dioxide with temperature compensation in power plant exhausts, Appl. Sci. 9 (2019) 442–456.
[32] J. Liu, Z. Du, Y. An, J. Li, D. Gao, K. Xu, Measurement of transient wavelength and line-width of DFB diode laser by delayed self-heterodyne interferometer, Proc. SPIE- Int. Soc. Opt. Eng. (2010).
[33] Z. Li, S. Yao, W. Lu, Study on temperature correction mothod of CO_2 measurement by TDLAS, Spectrosc. Spect. Anal. 38 (2017) 2048–2053.
[34] S. Wagner, B.T. Fisher, J.W. Fleming, V. Ebert, TDLAS-based in situ measurement of absolute acetylene concentrations in laminar 2D diffusion flames, P Combust. Inst. 32 (2009) 839–846.
[35] S. Wagner, M. Klein, T. Kathrotia, U. Riedel, T. Kissel, A. Dreizler, V. Ebert, Absolute, spatially resolved, in situ CO profiles in atmospheric laminar counter-flow diffusion flames using 2.3 μm TDLAS, Appl. Phys. B 109 (2012) 533–540.
[36] Z. Qu, J. Nwaboh, O. Werhahn, V. Ebert, Towards a dTDLAS-based spectrometer for absolute HCl measurements in combustion flue gases and a better evaluation of thermal boundary layer effects, Flow., Turbul. Combust. 106 (2021) 533–546.
[37] E. Schlosser, T. Fernholz, H. Teichert, V. Ebert, In situ detection of potassium atoms in high-temperature coal-combustion systems using near-infrared-diode lasers, Spectrochim. Acta Part A: Mol. Biomol. Spectrosc. 58 (2002) 2347–2359.
[38] E. Schlosser, J. Wolfrum, L. Hildebrandt, H. Seifert, B. Oser, V. Ebert, Diode laser based in situ detection of alkali atoms: development of a new method for determination of residence-time distribution in combustion plants, Appl. Phys. B: Lasers Opt. 75 (2002) 237–247.
[39] M. Chen, S. Xie, G. Zhou, D. Wei, H. Wu, S. Takahashi, H. Matsumoto, K. Takamasu, Absolute distance measurement based on spectral interferometer using the effect of the FSR of a Fabry–Perot etalon, Opt. Laser Eng. 123 (2019) 20–27.
[40] D.M. Marques, J.A. Guggenheim, R. Ansari, E.Z. Zhang, P.C. Beard, P.R.T. Munro, Modelling Fabry-Pérot etalons illuminated by focussed beams, Opt. Express 28 (2020) 7691.